

Self-collision of a portal wormhole

Justin C. Feng¹, José P. S. Lemos¹, and Richard A. Matzner²

¹*Centro de Astrofísica e Gravitação—CENTRA, Departamento de Física, Instituto Superior Técnico—IST, Universidade de Lisboa—UL, Av. Rovisco Pais 1, 1049-001 Lisboa, Portugal*

²*Theory Group and Center for Gravitational Physics, The University of Texas at Austin, Texas 78712, USA*



(Received 24 March 2021; accepted 7 May 2021; published 14 June 2021)

We consider the self-collision of portals in classical general relativity. Portals are wormholes supported by a single loop of negative mass cosmic string, and being wormholes, portals have a nontrivial topology. Portals can be constructed so that the curvature is zero everywhere outside the cosmic string, with vanishing ADM mass. The conical singularities of these wormholes can be smoothed, yielding a spatial topology of $S^2 \times S^1$ with a point corresponding to spatial infinity removed. If one attempts to collide the mouths of a smoothed portal to induce self-annihilation, one naively might think that a Euclidean topology is recovered, which would violate the classical no topology change theorems. We consider a particular limit of smoothed portals supported by an anisotropic fluid, and find that while the portal mouths do not experience an acceleration as they are brought close together, a curvature singularity forms in the limit that the separation distance vanishes. We find that in general relativity, the interaction between portal mouths is not primarily gravitational in nature, but depends critically on matter interactions.

DOI: [10.1103/PhysRevD.103.124037](https://doi.org/10.1103/PhysRevD.103.124037)

I. INTRODUCTION

A portal is a type of traversable wormhole described in [1] as a loop-based wormhole supported by a single loop of negative mass/negative tension cosmic string. Portals can be thought of as a limiting case of a spherical thin-shell wormhole that is flattened to a disk. Portals may be constructed so that the geometry is flat everywhere except at the string. The dihedral wormhole, the two-dimensional version of a polyhedral wormhole considered in [2], is an example of a portal (with corners). To construct a portal one can employ the thin-shell formalism to compute the energy-momentum tensor for the matter distribution required to hold it open. One finds that a tremendous amount of negative mass is needed to support portals of this type; a calculation in [1] estimates that a square-shaped dihedral wormhole [2] with a surface area of $\sim 1 \text{ m}^2$ requires a cosmic string on the wormhole boundary with a negative mass of the magnitude of the mass of Jupiter to hold it open. Portals may be obtained by taking limits of other spacetime geometries, such as the zero-mass limit for an appropriate analytic extension of the Kerr metric [3–5] (there, portals are referred to as gates); see also [6] which discusses similar wormhole structures in a class of spheroidal solutions to the vacuum Einstein equations. In this article, we adopt the terminology of [7,8] for portals since they are now widely known as such in popular culture due to examples found in media, for instance, those found in the eponymous video games [9].

Quantum gravitational considerations suggest that spacetime at the Planck scale may permit fluctuations in topology [10–12], so one might expect portal-like wormholes

to form during the Planck epoch of the early universe. In the case such wormholes are stable or metastable, cosmic inflation could expand them to macroscopic sizes [13]. Of course, whether portals or portal-like wormholes are stable depends on the microscopic description of the cosmic string required to support the portal. The locally defined mass for such a cosmic string is negative, so a microscopic model will necessarily violate energy conditions. More generally, it has been shown under some rather general considerations that traversable wormholes [14] require the violation of the null energy condition [15–17]; see also [1]. However, such a violation does not necessarily imply that a solution is unphysical. For instance, the avoidance of energy condition violations in the energy-momentum tensor for matter has been treated within modified gravity theories [18], and it has been shown that traversable wormhole solutions can be constructed in Einstein-Dirac-Maxwell theory, the fermionic sector of which violates the null energy condition [19]. For a detailed discussion of energy conditions, we refer to the review [20].

In this work, we consider the smoothing and self-collision of portals, assuming a simple matter model for the cosmic string. Being wormholes, portals have a nontrivial spatial topology. Indeed, we will construct smoothed portals and show that their topology in three spatial dimensions is $S^2 \times S^1$ minus a point corresponding to spatial infinity. For an axisymmetric portal configuration, one might imagine taking a limit in which the portal mouths are brought together in a manner in which one would

naively expect to recover a Euclidean topology. However, this would run contrary to classical no topology change theorems [21,22]. Such a limit is nonetheless useful for identifying and studying obstructions to topology change in classical general relativity, and may perhaps be of interest for studying topology-changing processes in quantum gravity. Furthermore, an understanding of the self-interaction of portals can (stability issues aside) shed some light on whether portals are expected to persist after the Planck epoch of the early universe.

In Sec. II, we describe the construction of portals. In Sec. III, we discuss the smoothing of the conical singularities in portals. In Sec. IV, we carefully illustrate the topology of smoothed portals. In Sec. V, a line element for static smoothed axisymmetric portals in cylindrical coordinates is constructed. In Sec. VI, junction conditions are analyzed. In Sec. VII, we examine the self-collision of portals. In Sec. VIII, we discuss results. Throughout this article, we consider a $3 + 1$ dimensional spacetime and employ the $(-, +, +, +)$ signature, choosing units such that the gravitational constant G and the speed of light are set to one, $G = 1$ and $c = 1$. Unless stated otherwise, all diagrams in this article are spatial, i.e., they describe the geometry and topology of spatial hypersurfaces.

II. PORTALS: CONSTRUCTION

Portals may be constructed by way of a cut-and-paste procedure along a pair of two-dimensional disks of radius a in flat three-dimensional Euclidean space. One can imagine portals as a limiting case of a spherical thin-shell wormhole that is flattened to a disk; the thin-shell formalism may then be employed to compute the energy-momentum tensor for the matter distribution required to hold it open.

Let both disks be centered on the z -axis, with disk 1 lying in the plane $z = z_0$ and disk 2 lying in the plane $z = -z_0$. The cut and paste procedure, as illustrated in Fig. 1, involves gluing the top face of disk 1, denoted by a_1 , to the bottom face of disk 2, denoted by a_2 , and gluing the bottom face of disk 1, denoted by b_1 , to the top face of disk 2, denoted by b_2 . The result is a portal wormhole, i.e., a portal. Such a wormhole is illustrated in Fig. 2, which also shows a curve that passes into the bottom face a_2 and emerges from the top face a_1 . In Fig. 3 a cut of the space through $y = 0$ is made and the two-dimensional x - z plane of the wormhole is shown embedded in a different three-dimensional Euclidean space. Note that to simplify the analysis, we shall only consider cases where the identifications are performed without twisting, meaning that a frame transported along a straight line traveling through the wormhole does not experience any change in orientation.

It is appropriate at this point to introduce some terminology. The surfaces of disk 1 and disk 2 will be referred to as the mouths of the wormhole w . The boundary of disks 1 and 2, which is really a single surface of codimension two,

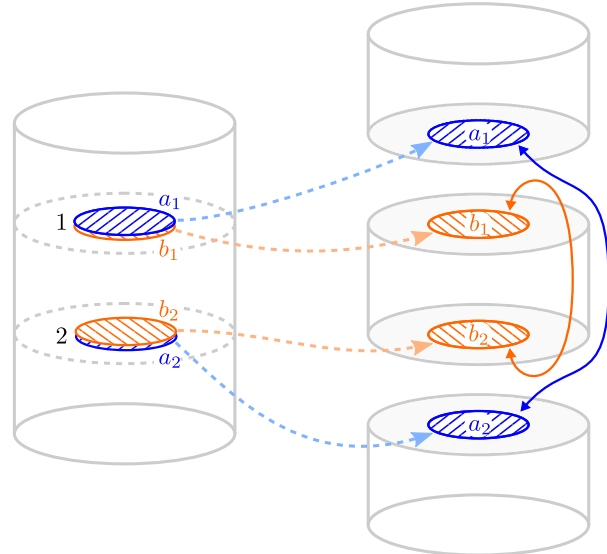


FIG. 1. Gluing procedure for axisymmetric portals. The left side of the diagram describes a cylindrical region in the three-dimensional Euclidean space centered on the z -axis. Disks 1 and 2 are on the respective planes defined by $z = z_0$ and $z = -z_0$, have radius a and are also centered on the z -axis. The right side of the diagram describes the gluing procedure for the disks, where one performs the identifications $a_1 \leftrightarrow a_2$, and $b_1 \leftrightarrow b_2$.

will be denoted ∂w and referred to as the wormhole boundary.

The wormhole boundary is singular, where we define singularities in terms of geodesic incompleteness [23], and in particular, we regard a singularity to be any (limit) point or submanifold through which one cannot extend a geodesic. The singularity here is rather mild; it is in fact a

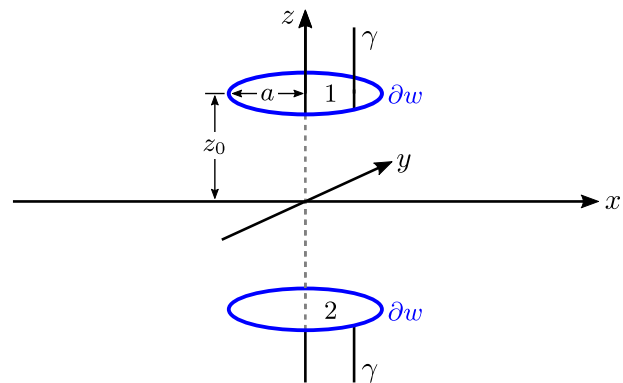


FIG. 2. Diagram of a portal in three-dimensional space, assumed Euclidean. The portal wormhole w has radius a and boundary denoted by ∂w . The curve γ is parallel to the z -axis. Observe that γ does not pass through the region $-z_0 < z < z_0$, $a \leq 1$. Though the boundary to the wormhole mouths ∂w appears in two places, it is in fact a single surface. Here the two previous blue and orange colors used in the identification process of the two sides of the portal are combined into a single blue color to simplify the figure.

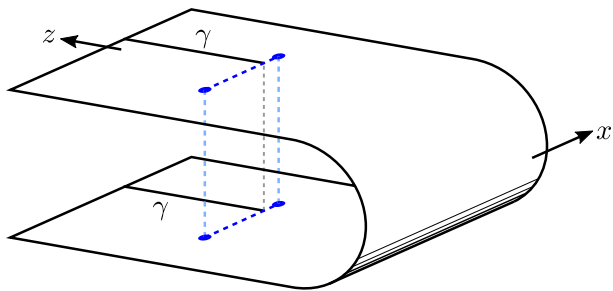
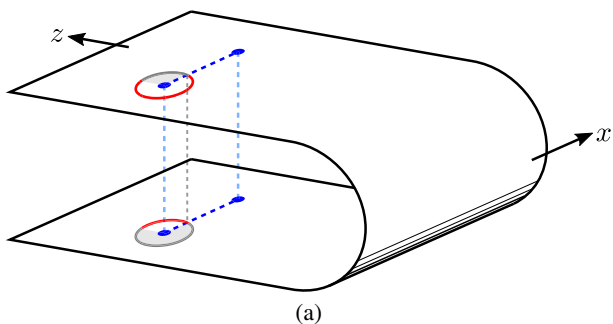
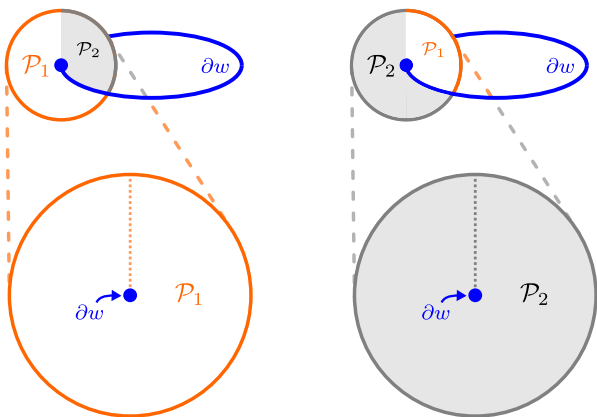


FIG. 3. An illustration of the x - z plane of Fig. 2, embedded in a different three-dimensional Euclidean space. Here, the vertical dotted lines have a proper distance of zero. Again, the two previous blue and orange colors used in the identification process of the two sides of the portal have been mixed into a single blue color.



(a)



(b)

FIG. 4. Illustration of surface \mathcal{P} in the neighborhood of ∂w . \mathcal{P} is defined to be the subset to a plane orthogonal to the tangent vectors of ∂w . In (a), \mathcal{P} is illustrated in the x - z plane as the region enclosed by the circle. In (b), the surface \mathcal{P} is a single surface divided into two regions labeled \mathcal{P}_1 and \mathcal{P}_2 . In the bottom portion of the diagram, \mathcal{P}_1 and \mathcal{P}_2 are illustrated as flat disks, which have a cut along the vertical half-dotted lines—they are glued together in the manner indicated in the top portion of (b) to form the surface \mathcal{P} . Again, the two previous blue and orange colors used in the identification process of the two sides of the portal have been given in blue.

conical singularity characterized by a surplus angle of 2π . To see this, consider Fig. 4, which describes the geometry surrounding the singularity in terms of a surface \mathcal{P} , which is a subset of a plane normal to the wormhole boundary ∂w . In particular, \mathcal{P} is defined to be a two-dimensional surface cutting through the wormhole boundary ∂w such that the tangent vector of ∂w is normal to the plane \mathcal{P} . In Fig. 4(a), \mathcal{P} is illustrated in the x - z plane as the region enclosed by the circle. From Fig. 4(b) one can infer that, excluding the singular point at ∂w , \mathcal{P} can be decomposed into two flat disks \mathcal{P}_1 and \mathcal{P}_2 which are each cut along a radial line and glued together along the cut lines such that the disk \mathcal{P}_2 is effectively inserted into the cut line of \mathcal{P}_1 ; the point ∂w in the surface \mathcal{P} may then be characterized by a surplus angle of 2π .

A glimpse of the self-collision problem, or the limit $z_0 \rightarrow 0$, can be now advanced. At first glance, the portal appears to annihilate itself, since it is naively expected that the wormhole approaches Euclidean space in this limit. However, being a wormhole, the topology of a portal is nontrivial, so the complete self-annihilation of a portal implies a change in the topology of the manifold. Such a process will likely be of interest for studying topology change in quantum gravity. A natural question, the answer to which forms one of the important topics of this article, is whether gravity encourages or obstructs the collision between the mouths of portals supported by smoothed cosmic strings.

III. SMOOTHED COSMIC STRINGS

The metric for a straight nonsingular cosmic string can be written in cylindrical coordinates (t, r, φ, ζ) as $ds^2 = -dt^2 + dr^2 + \alpha^2 r^2 d\varphi^2 + d\zeta^2$. For α different from unity this metric has a conical singularity at $r = 0$. To smooth this singularity out one introduces a function $\psi = \psi(r)$ such that the line element takes the form

$$ds^2 = -dt^2 + \psi dr^2 + \alpha^2 r^2 d\varphi^2 + d\zeta^2. \quad (1)$$

One may read off the components of the metric tensor $g_{\mu\nu}$ by comparison with $ds^2 = g_{\mu\nu} dx^\mu dx^\nu$. The string smoothing function ψ must satisfy the properties,

$$\lim_{r \rightarrow 0} \psi(r) = \alpha^2, \quad \lim_{r \rightarrow \infty} \psi(r) = 1. \quad (2)$$

For a fixed domain $0 < \varphi < 2\pi$, (with $\varphi = 0$ and $\varphi = 2\pi$ identified), $\alpha < 1$ corresponds to a line element for a conical spacetime in the limit $\psi \rightarrow 1$ with a deficit angle $\delta = 2\pi(1 - |\alpha|)$. For portals, the relevant parameter choice is $\alpha = 2$, which corresponds to a surplus angle of 2π in the singular limit $\psi \rightarrow 1$. The singular string is at $r = 0$; the smoothing should maintain the *core* of the string at $r = 0$, with possible shifts Δr much smaller than the width of the smoothing region.

One can evaluate the Einstein tensor $G_{\mu\nu}$ for the metric given in Eq. (1) which has the following nonvanishing components

$$\begin{aligned} G_{tt} &= -\frac{1}{2r} \frac{\partial}{\partial r} \left[\frac{1}{\psi} \right] \\ G_{\zeta\zeta} &= \frac{1}{2r} \frac{\partial}{\partial r} \left[\frac{1}{\psi} \right], \end{aligned} \quad (3)$$

so that $G_{\zeta\zeta} = -G_{tt}$. Combined with the Einstein field equations $G_{\mu\nu} = 8\pi T_{\mu\nu}$, where $T_{\mu\nu}$ is the energy-momentum tensor, this result suggests a rudimentary model for a negative mass cosmic string in general relativity: one may model a straight, negative mass cosmic string as a negative mass anisotropic fluid with energy momentum tensor $T_{..} = \text{diag}(\rho_e, p_r, p_\phi, p_\zeta)$ and equation of state $p_r = 0$, $p_\phi = 0$, and $p_\zeta = -\rho_e$, where $\rho_e < 0$, and with ρ_e being the energy density, and p_r , p_ϕ , and p_ζ , being the stresses in the respective directions. One might expect the equation of state $p_\zeta = -\rho_e$ to lead to instabilities, since one might generally expect systems containing negative energy matter to be unstable. However, these issues of instability concern the microscopic features of the cosmic string. For our purposes, this simple model, which we imagine to be a coarse-grained description of a cosmic string, suffices.

IV. TOPOLOGY OF SMOOTHED PORTALS

Now we consider the topology of a portal in a spatial slice. Since one can smooth out the conical singularities for cosmic strings, one can construct a manifold containing a portal that is everywhere regular. To simplify the discussion, we describe the topology in the context of the axisymmetric portal configuration as illustrated in Fig. 2.

Since we consider axisymmetric portals, the spatial topology can be represented as a slice along the x - z plane which upon compactification is illustrated in Fig. 5. In Fig. 5(a) a straightforward presentation of the compactified slice is shown; note that this diagram has cuts, indicated by the dotted lines between the contours a_i and b_i , $i \in \{1, 2\}$. In Fig. 5(b) a different, more elaborate but interesting presentation of the compactified manifold without cuts is shown. That Figs. 5(a) and 5(b) describe the same manifold can be seen by recognizing that regions I and II in Fig. 5(a) are homeomorphic to their respective counterparts in Fig. 5(b), and that the labeled segments of the boundaries enclosing regions I and II are glued together in the same way in Figs. 5(a) and 5(b).

Figure 6 is a schematic image of Fig. 5, and is helpful for understanding the topology of the portal. From it, one can infer the three-dimensional topology by recognizing that the possible curves σ^i which could be drawn on Fig. 5(a) and are displayed explicitly in Fig. 6(a), indeed represent surfaces with the topology of a two-sphere S^2 . Moreover, the same curves that could be drawn on Fig. 5(b) are displayed

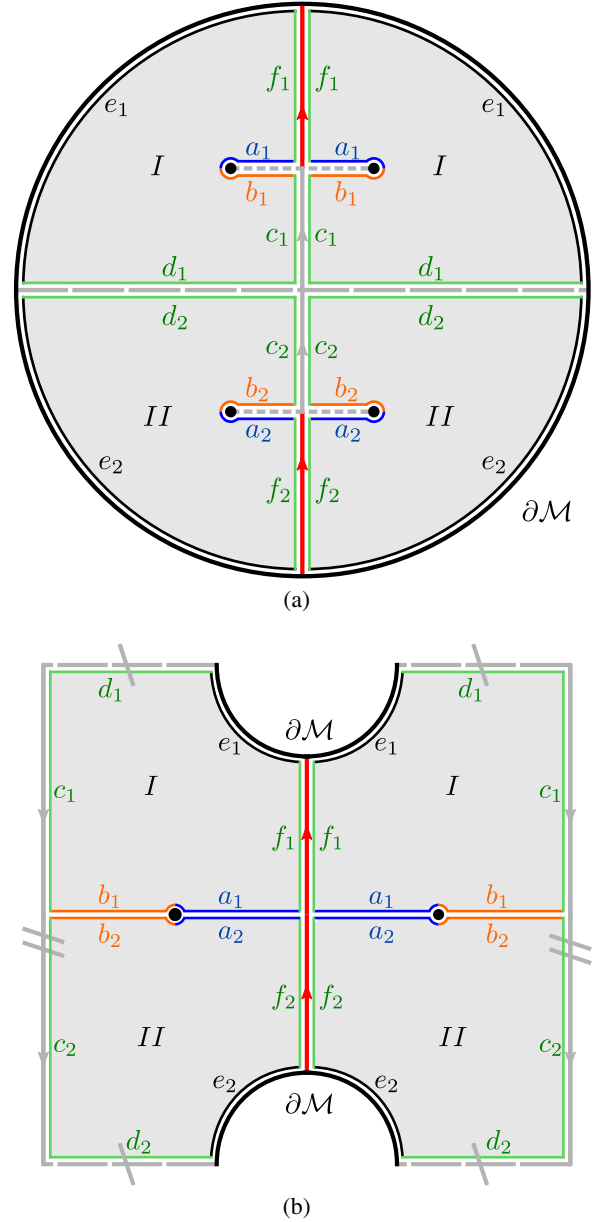


FIG. 5. Topology of a portal. (a) describes the compactified x - z plane of the axisymmetric portal of Fig. 2, with $\partial\mathcal{M}$ being the boundary at $\tilde{r} = \sqrt{x^2 + z^2} = \infty$. Here, the dotted lines (representing the mouths of the wormhole) denote cuts in the manifold, and the vertical line in the center corresponds to the z -axis. (b) is an illustration of the same compactified plane, with the vertical and horizontal sides identified. The contours enclosing the shaded regions I and II form the boundaries of I and II, and their segments are labeled to illustrate the correspondence between the diagrams. The segments labeled c_1, c_2, f_1, f_2 all lie along the z -axis, and the segments e_1 and e_2 lie along the boundary $\partial\mathcal{M}$. The remaining segments are glued: a_1 is glued to a_2 , b_1 is glued to b_2 , and d_1 is glued to d_2 .

in Fig. 6(b), now appearing as horizontal lines. The identifications indicate a topology $S^2 \times S^1$ with a point (or sphere-shaped hole) corresponding to spatial infinity $\partial\mathcal{M}$,

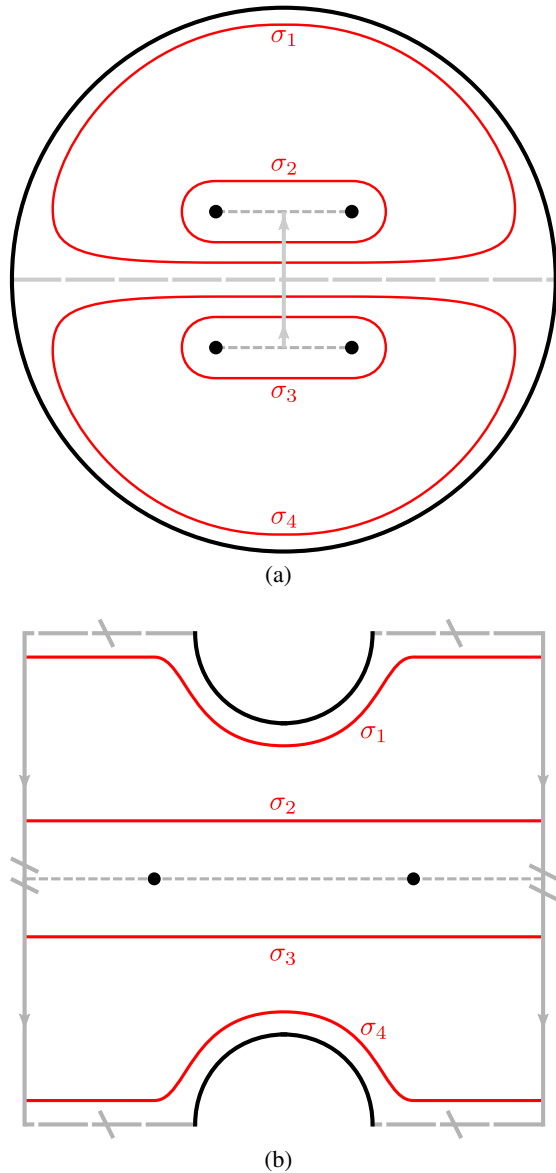


FIG. 6. Behavior of surfaces in Fig. 5. Since (a) is a representation of an axisymmetric configuration, one can imagine rotating (a) about a vertical line in the center so that the contours here represented by σ_1 , σ_2 , σ_3 , and σ_4 , all describe surfaces with topology S^2 . Since the vertical gray lines in (b) are identified [these correspond to the vertical gray line in the center of (a)], one can then infer that the topology is $S^2 \times S^1$ minus a point or minus a hole.

which is represented by the semicircular arcs in Figs. 5(b) and 6(b).

As an aside, we remark on the relationship of the construction performed here to the Deutsch-Politzer (DP) time machine, which is constructed by way of a similar cut-and-paste procedure in n -dimensional spacetime [24–27]. In particular, the $2 + 1$ counterpart of the DP spacetime can be easily visualized by replacing the z -axis in Fig. 2 with

the t -axis. As a further aside, one might also imagine an interesting variant of the DP construction in which the mouths are placed side by side. In particular, one can in four-dimensional Minkowski space perform a cut-and-paste procedure on the $t = 0$ slice along two nonoverlapping regions s_1 and s_2 , each bounded by a two-sphere of the same radius, such that timelike and null curves passing through s_1 from $t < 0$ emerge through s_2 at $t > 0$. Such a construction is homeomorphic to the DP spacetime (though having a different causal structure, lacking closed timelike curves), and might be thought of as describing a form of teleportation in which two regions of space effectively switch places—for this reason, it may be appropriate to refer to them as *teleporters*. The topology of DP spacetimes (and teleporters, since they are homeomorphic) in n dimensions is $S^{n-1} \times S^1$ minus a point corresponding to infinity [26,27], which for $n = 3$ is the same as the spatial topology of the portals considered here. However, it was also shown in [26,27] that one cannot construct an everywhere smooth metric of Lorentzian signature on these spacetimes, in contrast to the smooth Euclidean signature metrics we will construct in this paper. Moreover, though the spacelike quasiregular singularities of teleporters and DP spacetimes resemble those of conical singularities, they differ in that spacelike quasiregular singularities can significantly alter the causal structure of spacetime in the vicinity of the singularity—see in particular Fig. 3 of [28]. For this reason, one cannot regard teleporters and DP spacetimes as limits of smooth spacetimes, making them difficult to study within the framework of classical general relativity. Note that though one might imagine that the formation of spacelike quasiregular singularities is forbidden by some physical principle, the formulation of such a principle (beyond excluding by fiat those singularities) can be a rather subtle matter, as discussed in [29,30].

V. STATIC LINE ELEMENT FOR PORTAL GEOMETRIES

Before a proper analysis of the self-interaction and self-collision of a portal can be conducted, it is appropriate to specify coordinates which are simple in Fig. 5(a) and regular everywhere in Fig. 5(b) except for a surface of codimension one, which is dealt with later when transforming to cylindrical coordinates. To do this, we consider the configuration illustrated in Fig. 2 in the singular limit where the manifold is everywhere flat except for the conical singularity at the wormhole boundary ∂w , i.e., the string core. Assume ∂w is circular, with a radius a , centered on the z -axis at $\pm z_0$. It is natural to consider as a starting point oblate spheroidal coordinates in the $z > 0$ region, with ∂w as the focal ring. In ordinary Euclidean space, spheroidal coordinates centered on ∂w at $z = +z_0$ are related to Cartesian coordinates in the following manner:

$$\begin{aligned}
x &= a \cosh \mu \cos \nu \cos \phi, \\
y &= a \cosh \mu \cos \nu \sin \phi, \\
z &= z_0 + a \sinh \mu \sin \nu.
\end{aligned} \tag{4}$$

A reflection about the $z = 0$ plane yields a coordinate system that is regular everywhere except for a measure zero set which includes the focal rings at ∂w and the $z = 0$ plane, where the coordinates fail to be smooth. One can then apply junction conditions to deal with the nonregularity of the coordinate system at $z = 0$. The line element for Minkowski spacetime in spheroidal coordinates takes the form

$$\begin{aligned}
ds^2 &= -dt^2 + \frac{1}{2} a^2 (\cosh 2\mu - \cos 2\nu) (d\mu^2 + d\nu^2) \\
&\quad + a^2 \cosh^2 \mu \cos^2 \nu d\phi^2,
\end{aligned} \tag{5}$$

A second order expansion about $\mu = 0, \nu = 0$ of the second term yields $\frac{1}{2} a^2 (\cosh 2\mu - \cos 2\nu) \approx a^2 (\mu^2 + \nu^2)$. Similarly expanding the third term yields $a^2 \cosh^2 \mu \cos^2 \nu \approx a^2 (1 + \mu^2 - \nu^2)$ with \approx denoting the expansion to second order. Note that $\mu = 0, \nu = 0$ corresponds to the position of the focal ring. For large a , one may restrict to a small angular range in ϕ , and neglect terms $\mu^2 d\phi^2$ and $\nu^2 d\phi^2$. This corresponds to a limit in which one can neglect the curvature of the wormhole boundary. In this limit, the line element has the form:

$$ds^2 \approx -dt^2 + a^2 (\mu^2 + \nu^2) (d\mu^2 + d\nu^2) + a^2 d\phi^2. \tag{6}$$

It is straightforward to verify that this is in fact a flat metric everywhere except at the origin point $\mu = 0, \nu = 0$. It turns out that one can recover the conical metric given in Eq. (1) in the limit $\psi \rightarrow 1$ for $\alpha = 2$ with the coordinate choice given by $\mu = \sqrt{\frac{2r}{a}} \sin \varphi$ and $\nu = \sqrt{\frac{2r}{a}} \cos \varphi$ which yields $ds^2 \approx -dt^2 + dr^2 + 4r^2 d\varphi^2 + a^2 d\phi^2$. This result indicates that the geometry immediately surrounding the conical singularity of the singular portal is given by the metric given in Eq. (6) if one extends the domain of the coordinates μ and ν to negative values. It is straightforward to work out the following differential expressions

$$\begin{aligned}
dr &= a(\mu d\mu + \nu d\nu), \\
2rd\varphi &= a(\nu d\mu - \mu d\nu),
\end{aligned} \tag{7}$$

where $r = \frac{a}{2} (\mu^2 + \nu^2)$ and $\tan \varphi = \frac{\mu}{\nu}$. One can then use the differentials in Eq. (1) to smooth out the conical singularities, resulting in the line element

$$\begin{aligned}
ds^2 &\approx -dt^2 + a^2 (\mu^2 + \nu^2) (d\mu^2 + d\nu^2) + a^2 d\phi^2 \\
&\quad + a^2 (\psi - 1) (\mu d\mu + \nu d\nu)^2.
\end{aligned} \tag{8}$$

When the string smoothing function is trivial, i.e., $\psi = 1$, one recovers Eq. (6). We note that here, the point $\mu = \nu = 0$ corresponds to the core of the smoothed string ($r = 0$), about which the string smoothing function is centered.

The analysis so far requires small values for μ and ν and a restriction to a small angular range in ϕ . However, Eq. (8) can be used to motivate a line element suitable for a larger range of coordinate values. Since μ is a hyperbolic coordinate, and ν is an angular coordinate, it is natural to replace instances of μ and ν in the Taylor-expanded line element (8) with the appropriate hyperbolic and trigonometric functions. Choosing

$$r = \frac{a}{4} (\cosh 2\mu - \cos 2\nu) \tag{9}$$

(note that $r = 0$ at the core of the string), one may then construct the line element

$$\begin{aligned}
ds^2 &= -dt^2 + \frac{1}{2} a^2 (\cosh 2\mu - \cos 2\nu) (d\mu^2 + d\nu^2) \\
&\quad + a^2 \cosh^2 \mu \cos^2 \nu d\phi^2 \\
&\quad + a^2 (\psi - 1) (\sinh \mu d\mu + \sin \nu d\nu)^2,
\end{aligned} \tag{10}$$

and it can be verified that this line element reduces to Eq. (8) in the appropriate limits.

It is convenient to transform Eq. (10) back to Cartesian coordinates, since the properties of the boundary surface $z = 0$, which corresponds to the constraint (recall z_0 is half the z separation between the portal mouths)

$$\sinh \mu \sin \nu = -\frac{z_0}{a}, \tag{11}$$

are of particular interest for the self-collision problem. In fact, since the problem is axially symmetric, it is more convenient to transform to the cylindrical coordinates ρ, ϕ, z , where one has the coordinate definition $\rho := a \cosh \mu \cos \nu$, and z is defined in Eq. (4). One can verify that in this cylindrical coordinate system, the line element (10) takes the form

$$\begin{aligned}
ds^2 &= -dt^2 + d\rho^2 + \rho^2 d\phi^2 + dz^2 \\
&\quad + \frac{\Psi(\rho, z) - 1}{\Delta z^2 + \Delta \rho^2} [\Delta \rho d\rho + \Delta z dz]^2,
\end{aligned} \tag{12}$$

where $\Psi(\rho, z) = \psi(r)$ is the string smoothing function, with r being given by

$$r = \frac{\sqrt{(\Delta \rho^2 + \Delta z^2)[(2a + \Delta \rho)^2 + \Delta z^2]}}{2a}, \tag{13}$$

and the following have been defined

$$\begin{aligned}\Delta\rho &:= \rho - a, \\ \Delta z &:= z - z_0.\end{aligned}\quad (14)$$

In these coordinates, the core ($r = 0$) of the smoothed string is located at $\Delta\rho = \Delta z = 0$. We compute the Einstein tensor for Eq. (12) to leading order in a^{-1} , assuming $\Delta\rho \ll a$, and that $\Psi(\rho, z)$ and its derivatives are of order unity for large a . The nonvanishing components of the Einstein tensor take the form:

$$\begin{aligned}G^t_t &= \mathcal{G} + \mathcal{O}(a^{-1}) \\ G^\rho_\rho &= \mathcal{O}(a^{-1}) \\ G^\phi_\phi &= \mathcal{G} + \mathcal{O}(a^{-1}) \\ G^z_z &= \mathcal{O}(a^{-1}) \\ G^\rho_z &= G^z_\rho = \mathcal{O}(a^{-1}),\end{aligned}\quad (15)$$

where $\mathcal{G} = \mathcal{G}(\Delta\rho, \Delta z)$ is given by:

$$\begin{aligned}\mathcal{G} &= \frac{1}{4\Psi^2(\Delta\rho^2 + \Delta z^2)} \\ &\times \{-2\Delta z[1 + \Psi - \Delta\rho\partial_\rho\Psi]\partial_z\Psi - \Delta\rho^2\partial_z\Psi^2 \\ &- [2\Delta\rho(1 + \Psi)\partial_\rho\Psi + \Delta z^2(\partial_\rho\Psi)^2] \\ &+ 2\Psi[\Delta z^2\partial_\rho^2\Psi + \Psi\Delta\rho^2\partial_z^2\Psi - 2\Delta\rho\Delta z\partial_z\partial_\rho\Psi]\}.\end{aligned}\quad (16)$$

As expected, we recover the Einstein tensor of Eq. (3) in the limit of large a , so in this limit, the model of the cosmic string as an anisotropic fluid with equation of state $p_\zeta = -\rho_e$ applies. Of course, for finite a , when the curvature of the cosmic string becomes significant, a more complicated matter model will be needed.

VI. JUNCTION CONDITIONS

A. Thin shell at $z=0$

The line element given in Eq. (12) is only valid for $z > 0$. However, we can construct a metric for the $z < 0$ region simply by reflecting in the plane $z = 0$, which is depicted by the shaded region in Fig. 7. In general, such a procedure will create a thin shell at the $z = 0$ surface. For singular (non-smoothed) strings, the space is 3-flat, except at the locations of the strings. Thus although there might be a coordinate discontinuity at the $z = 0$ plane, there would be no geometrical singularity. However, the situation is different for smoothed portals, since the smoothing of the string produces a ‘‘fattened’’ matter distribution which can extend to the $z = 0$ surface.

To see that a thin shell is created under a reflection about $z = 0$, we employ the thin shell formalism [31,32] to compute the surface stress tensor at $z = 0$ (here the indices i, j correspond to the coordinates t, ρ, ϕ):

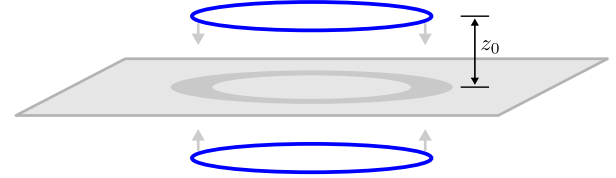


FIG. 7. An illustration of the self-collision problem. The $z = 0$ plane has been shaded in gray. Equation (18) indicates that a generic smoothing of the string (defined by a choice for Ψ) will generate a thin shell at the $z = 0$ plane. For a smoothed string of a given thickness, one expects the energy of the shell to be concentrated in a circular strip (indicated in dark gray) centered at $\rho = a$.

$$\tau_{ij} = -\frac{1}{8\pi}([K_{ij}] - [K]\gamma_{ij}),\quad (17)$$

where K_{ij} is the extrinsic curvature tensor of the surface $z = 0$, which is given by the expression $K_{ij} = \frac{1}{2\alpha}(\frac{\partial\gamma_{ij}}{\partial z} - D_i\beta_j - D_j\beta_i)$, where D_i is the surface covariant derivative compatible with the induced metric $\gamma_{ij} = g_{ij}$, $\beta_i := g_{zi}$, $\alpha = \sqrt{|\frac{g}{\gamma}|}$, with g and γ being the determinants of the respective metric tensors $g_{\mu\nu}$ and γ_{ij} , and the brackets $[A] := A_+ - A_-$ denote a jump in the extrinsic curvatures. The extrinsic curvatures are defined such that the unit normal vectors point in the same direction across the surface. Due to the symmetry in the problem, a nonvanishing extrinsic curvature will generally lead to a nonvanishing jump so that $[K_{ij}] = 2K_{ij}$ and $[K] = 2K$, resulting in a nonvanishing surface energy-momentum tensor τ_{ij} . A nonvanishing τ_{ij} describes the surface stress-energy of a thin shell at the $z = 0$ surface, as illustrated in Fig. 7.

Given the line element Eq. (12) for $z > 0$, and demanding that the geometry be symmetric about $z = 0$, the nonvanishing components of the surface energy-momentum tensor [given by (17)] take the form

$$\begin{aligned}\tau^t_t &= \tau^\rho_\rho + \tau^\phi_\phi, \\ \tau^\rho_\rho &= \frac{\Delta\rho(\Psi - 1)z_0}{4\pi(a + \Delta\rho)\sqrt{\Psi(\Delta\rho^2 + z_0^2)(\Delta\rho^2\Psi + z_0^2)}}, \\ \tau^\phi_\phi &= \frac{1}{8\pi\sqrt{\Psi(\Delta\rho^2 + z_0^2)(\Delta\rho^2\Psi + z_0^2)^{3/2}}}\{2(\Psi - 1)z_0^3 \\ &+ \Delta\rho z_0(\Delta\rho^2(\Psi + 1) + 2z_0^2)\partial_\rho\Psi \\ &+ \Delta\rho^2(\Delta\rho^2\Psi + z_0^2)\partial_z\Psi\},\end{aligned}\quad (18)$$

where Ψ and its derivatives are evaluated at $z = 0$, and mixed index components are presented due to their simplicity. The final expression for the components of τ^i_j depends on the choice of a string smoothing function, and vanishes where $\Psi = 1$ and $\partial_z\Psi = \partial_\rho\Psi = 0$, outside the

smoothing region. We note that τ^ρ vanishes regardless, in the large a limit.

B. Junction conditions at $z=0$

The shell at $z=0$ is somewhat artificial, as it is the consequence of a reflection about the $z=0$ plane. To eliminate this shell, we impose junction conditions, which amounts to the demand that $\tau^i_j = 0$. These junction conditions will lead to boundary conditions on the string smoothing function Ψ and its derivatives at $z=0$. Earlier, we saw that $\tau^i_j = 0$ if $\Psi = 1$ and $\partial_z \Psi = \partial_\rho \Psi = 0$, but here we show that for finite a , these boundary conditions follow from $\tau^i_j = 0$. From Eq. (18), we note that if $\tau^\rho_\rho = 0$ and $\tau^\phi_\phi = 0$, then $\tau^t_t = 0$. The vanishing of τ^ρ_ρ (assuming finite a) requires $\Psi|_{z=0} = 1$, which in turn implies $\partial_\rho \Psi|_{z=0} = 0$. Under these conditions, the vanishing of τ^ϕ_ϕ requires $\partial_z \Psi|_{z=0} = 0$. Thus, we can eliminate the shell by requiring the boundary conditions $\Psi = 1$, $\partial_\rho \Psi = 0$, and $\partial_z \Psi = 0$ at the $z=0$ surface.

In the large a limit, one can see from Eqs. (18) that $\tau^\rho_\rho \rightarrow 0$, so perhaps one can in this limit relax the condition $\Psi = 1$ at $z=0$. From Eq. (18), we find that the condition $\tau^t_t = \tau^\phi_\phi = 0$ yields the following differential equation for $\Psi|_{z=0}$:

$$\partial_\rho \Psi = -\frac{(\Delta\rho^4 \Psi + \Delta\rho^2 z_0^2) \partial_z \Psi + 2(\Psi - 1) z_0^3}{2\Delta\rho z_0^3 + \Delta\rho^3 (\Psi + 1) z_0}, \quad (19)$$

with the understanding that all quantities here are evaluated at $z=0$ and are at most functions of ρ . The right hand side of Eq. (19) can be expanded in $\Delta\rho$, under the assumption that Ψ and $\partial_z \Psi$ do not diverge at $\Delta\rho = 0$, yielding:

$$\partial_\rho \Psi = \frac{1 - \Psi}{\Delta\rho} + O(\Delta\rho). \quad (20)$$

If we require $\partial_\rho \Psi$ to be zero or finite at $z=0$ and $\Delta\rho = 0$, then $(\Psi - 1)|_{z=0} \propto \Delta\rho$, and it follows that at $z=0$ and $\Delta\rho = 0$, one must have $\Psi \rightarrow 1$.

C. Example smoothing function

It is not too difficult to construct a string smoothing function satisfying the finite a boundary conditions $\Psi = 1$, $\partial_\rho \Psi = \partial_z \Psi = 0$ at the $z=0$ surface. As an example, one may start with the following smoothing function ψ [33]:

$$\psi = \frac{r^2 + \bar{\alpha}^2 \varepsilon^2}{r^2 + \varepsilon^2}, \quad (21)$$

where $\bar{\alpha}$ has the value 2 for a smoothed cosmic string with surplus angle 2π at large r , and ε is roughly the thickness of the smoothed cosmic string. From ψ , one can construct a string smoothing function Ψ satisfying the boundary

conditions by promoting the quantity $\bar{\alpha}$ to a function of z of the form:

$$\bar{\alpha}\left(\frac{z}{z_0}\right) = \alpha + (1 - \alpha) \frac{\Omega\left(\frac{z}{z_0}\right)}{\Omega(0)}, \quad (22)$$

where $\alpha = 2$ for the portal geometry, and the function $\Omega(x)$ satisfies the properties

$$\begin{aligned} \Omega'(0) &= \Omega(1) = 0, \\ \Omega(0) &\neq 0, \\ \Omega(\infty) &= 0. \end{aligned} \quad (23)$$

These properties are constructed to ensure that $\bar{\alpha} = 2$ at $\rho = a$ and $z = z_0$; this condition is needed to avoid an additional conical singularity.

VII. DYNAMICAL PORTALS AND SELF-COLLISION

A. The self-collision problem

The self-collision problem for an axisymmetric portal can be understood with the help of Fig. 7. Here, we consider symmetry about $z=0$. As remarked earlier, the self-collision problem refers to a process in which the portal mouths are brought together, and corresponds to the limit $z_0 \rightarrow 0$. It may be useful to provide a conceptualization of the self-collision problem in the context of Fig. 5. One might imagine the self-collision of a portal as a process that brings together a portion of the top and bottom faces of Fig. 5(b). In particular, the outermost portions of the segments d_1 and d_2 in Fig. 5(b) are pinched together with segments b_1 and b_2 to make the left and right edges (segments c_1 and c_2) disappear. Alternatively, the distances, as defined by the spatial metric, along a subclass of curves that pass through the contours b_1, b_2 vanish.

To study the self-collision problem, we will consider a dynamical portal geometry in the large a limit and solve the Einstein field equations in $3+1$ form in the vicinity of an initial slice satisfying a generalization of the line element in Eq. (12). The goal of this calculation is to determine the acceleration of the portal mouths for a given set of initial data. For the matter model, we consider an anisotropic fluid with no stresses in the direction perpendicular to the length along the string, as indicated in Eq. (3); in doing so, we ignore matter interactions in the directions perpendicular to the string and highlight gravitational interactions between the portal mouths.

B. Time dependent metric

Here, we consider the large a limit. To simplify the notation, we make the replacements $\rho \rightarrow a$ and $\Delta\rho \rightarrow \bar{\rho}$. Without loss of generality, one may restrict to Gaussian normal coordinates in a neighborhood of the $t=0$ slice. We generalize the line element in Eq. (12) to the form:

$$ds^2 = -dt^2 + d\bar{\rho}^2 + a^2 d\phi^2 + dz^2 + \frac{\Psi - 1}{\chi^2 \Delta z^2 + \bar{\rho}^2} \times [\lambda^2 d\rho^2 + 2\chi\bar{\rho}\Delta z d\bar{\rho}dz + \chi^2 \Delta z^2 dz^2], \quad (24)$$

where now $\Psi = \Psi(\bar{\rho}, z, t)$, $\chi = \chi(\bar{\rho}, z, t)$, and $\lambda = \lambda(\bar{\rho}, z, t)$ are smooth functions of $\bar{\rho}$ and z . To ensure that the geometry is locally flat at the core of the string $\bar{\rho} = 0$, $z = z_0$, we require that $\Psi(0, z_0, 0) = 4$, $\chi(0, z_0, 0) = 1$, and $\lambda(\bar{\rho}, z_0, 0) = \bar{\rho}$; notice that the line element reduces to the form of Eq. (12) at the core of the string $\bar{\rho} = \Delta z = 0$. It is also appropriate to choose initial data such that $\dot{\Psi} = \dot{\chi} = \dot{\lambda} = 0$ at the core of the string, so the locally flat condition is maintained, at least to first order in time. To simplify the analysis, we will choose initial data such that at $\bar{\rho} = 0$, the quantity Ψ has a vanishing first derivative with respect to $\bar{\rho}$.

C. Geodesic distance between portal mouths

Here, we consider the length of a spatial geodesic connecting the cores of the smoothed strings supporting the portal mouths. The core of the string is defined to be $\bar{\rho} = 0$, $\Delta z = 0$ for $z > 0$, and the symmetric statement for $z < 0$. For the spatial part ($dt = 0$) of the line element in Eq. (24), one may verify that for a tangent vector $v = (0, 0, v^z)$, ${}^{(3)}\Gamma_{jk}^i v^j v^k \propto v^i$ at $\bar{\rho} = 0$ provided that $\partial_{\bar{\rho}} \Psi|_{\bar{\rho}=0} = 0$, which follows our choice of initial data along $\bar{\rho} = 0$. Thus, the line $\bar{\rho} = 0$, $\phi = \text{constant}$ is a spatial geodesic. Along this geodesic, the spatial part of the line element (24) simplifies to $ds^2 = \Psi dz^2$, so that the length L of the geodesic connecting the centers of the smoothed strings is given by the integral:

$$L = 2 \int_0^{z_0} \sqrt{\Psi} dz = L_0 + V_0 t + \frac{A_0}{2} t^2 + O(t^3). \quad (25)$$

The initial distance L_0 , the initial velocity V_0 and the initial acceleration A_0 may be obtained by expanding Ψ in t , with the following result:

$$\begin{aligned} L_0 &:= 2 \int_0^{z_0} \sqrt{\Psi_0} dz, \\ V_0 &:= \int_0^{z_0} \frac{\dot{\Psi}_0}{\sqrt{\Psi_0}} dz, \\ A_0 &:= \int_0^{z_0} \frac{2\Psi_0 \ddot{\Psi}_0 - \dot{\Psi}_0^2}{2\Psi_0^{3/2}} dz, \end{aligned} \quad (26)$$

where the subscripts 0 denote evaluation at $t = 0$, overdots denote derivatives with respect to t , and all quantities are understood to be evaluated at $\bar{\rho} = 0$. Since we are working in Gaussian normal coordinates, the velocity and acceleration are measured according to observers aligned with $\frac{\partial}{\partial t}$. This result indicates that if $\partial_{\bar{\rho}} \Psi|_{\bar{\rho}=0} = 0$ is assumed, one

only needs to know Ψ and its first and second time derivatives at $\bar{\rho} = 0$ to obtain the acceleration A_0 (L_0 and V_0 are determined by the initial data).

D. Anisotropic fluid

For the matter model, we consider an anisotropic fluid with an energy-momentum tensor of the form:

$$T_{\mu\nu} = \rho_u (u_\mu u_\nu - w_\mu w_\nu) \quad (27)$$

where ρ_u is the rest frame energy, u^μ is a unit timelike vector and w^μ is a unit spacelike vector. We choose them to have the following form:

$$\begin{aligned} u &= (u^t, u^{\bar{\rho}}, 0, u^z) \\ w &= \left(0, 0, \frac{1}{a}, 0\right) \end{aligned} \quad (28)$$

where the component u^t of the four-velocity is fixed by the normalization condition. The initial conditions for $u^{\bar{\rho}}$ and u^z will be discussed in the next section.

E. 3+1 equations and their solution

We will work in the 3+1 formalism, assuming Gaussian normal coordinates which correspond to the conditions $g_{tt} = -1$ and $g_{ti} = 0$. Here, the spatial metric will be denoted $\gamma_{ij} = g_{ij}$ to avoid confusion. In Gaussian normal coordinates, the 3+1 decomposition [34–36] of the Einstein field equations takes the form:

$$\dot{\gamma}_{ij} = 2K_{ij}, \quad (29)$$

$$\dot{K}_{ij} = 2K_{ik} K_j^k - K K_{ij} - {}^3R_{ij} - \kappa \left[\frac{1}{2} (S - \rho_m) \gamma_{ij} - S_{ij} \right], \quad (30)$$

$$D_k (K_i^k - \gamma_i^k K) = \kappa S_i, \quad (31)$$

$${}^3R + K^2 - K^{ij} K_{ij} = 2\kappa \rho_m, \quad (32)$$

where $\kappa = 8\pi$ (setting $G = c = 1$), K_{ij} is the extrinsic curvature, $\rho_m := T_{tt}$ is the energy density defined with respect to Gaussian normal observers, $S_{ij} = T_{ij}$ are the purely spatial components of the energy-momentum tensor (with trace $S := \gamma^{ij} S_{ij}$), $S_i := T_{ti}$ is the momentum density, ${}^3R_{ij}$ is the spatial Ricci tensor, and 3R its trace. Equations (31) and (32) are constraints on the initial data, and are referred to respectively as the momentum and Hamiltonian constraints. The time evolution of the system is provided by Eqs. (29) and (30).

First, we consider the constraints. The momentum constraint can in principle be solved for the fluid velocity components $u^{\bar{\rho}}$ and u^z but the constraint is quartic in $u^{\bar{\rho}}$ and

u^z . However, in the $\bar{\rho} \rightarrow 0$ limit, one component of the momentum constraint equation reads:

$$\frac{\Delta z^2 \rho_u u^{\bar{\rho}} \chi^2 \sqrt{\Delta z^2 (u^{\bar{\rho}})^2 \chi^2 + \Delta z^2 \chi^2 [(u^z)^2 \Psi + 1]}}{(\Delta z^2 \chi^2)^{3/2}} = 0, \quad (33)$$

which implies $u^{\bar{\rho}} = 0$ at $\bar{\rho} = 0$. We therefore require $u^{\bar{\rho}} \propto \bar{\rho}$. The Hamiltonian constraint given in (32) can be solved for the fluid density ρ_u [see Eq. (27)], bearing in mind $\rho_m = T_{tt}$.

We now turn to the evolution equations. For the purposes of this article, it suffices to compute the second time derivatives $\ddot{\Psi}$, $\ddot{\chi}$, $\ddot{\lambda}$ at $t = 0$ and $\bar{\rho} = 0$, given some specification for the initial data Ψ , χ , λ and $\dot{\Psi}$, $\dot{\chi}$, $\dot{\lambda}$. At the $t = 0$ surface, the extrinsic curvature K_{ij} may be computed by taking the time derivative of γ_{ij} ; its time derivative $\partial_t K_{ij}$ may be computed similarly. One finds that each term in Eq. (30) has the same matrix form:

$$M = \begin{bmatrix} a & 0 & b \\ 0 & 0 & 0 \\ b & 0 & c \end{bmatrix}, \quad (34)$$

so that there are three independent equations for $\ddot{\Psi}_0, \ddot{\chi}_0, \ddot{\lambda}_0$. In the $\bar{\rho} \rightarrow 0$ limit, the equations yield the following expressions (the details of the calculation are provided in the associated *Mathematica* file [37]):

$$\begin{aligned} \ddot{\Psi}_0 &= \frac{\dot{\Psi}^2}{2\Psi}, \\ \ddot{\chi}_0 &= \frac{\dot{\chi}}{2} \left[\frac{4\dot{\chi}}{\chi} + \left(\frac{1}{\Psi} - \frac{4}{\Psi-1} \right) \dot{\Psi} \right] - \frac{3R\Delta z \chi^2 \Psi u^z \partial_{\bar{\rho}} u^{\bar{\rho}}}{(\Psi-1)[1+(u^z)^2\Psi]}, \\ \ddot{\lambda}_0 &= \dot{\lambda} \left[\frac{4\dot{\chi}}{\chi} - \frac{2\dot{\Psi}}{\Psi-1} - \frac{(u^z)^2 \dot{\Psi}}{2(u^z)^2\Psi+2} \right]. \end{aligned} \quad (35)$$

These equations are subject to the condition:

$$\dot{\lambda}_0 = \frac{\Delta z \chi \sqrt{-3R\Psi u^z}}{\sqrt{2(\Psi-1)((u^z)^2\Psi+1)}}, \quad (36)$$

which assumes ${}^3R < 0$ (this is the case if K and $\rho_m < 0$ dominate in the Hamiltonian constraint) and is needed to ensure that $\dot{\lambda}_0$ remains finite at $\bar{\rho} = 0$. That an additional constraint on $\dot{\lambda}_0$ is needed should not be surprising, as we have already solved the Hamiltonian and momentum constraints, and have fixed the gauge in choosing Gaussian normal coordinates. It is well-known that general relativity has two physical degrees of freedom, and since there are three functions in the metric, one might expect the equations to yield an additional constraint. We note that if $\dot{\Psi} = \dot{\chi} = \dot{\lambda} = \Delta z = 0$, Eq. (35) implies $\ddot{\Psi} = \ddot{\chi} = \ddot{\lambda} = 0$. For the appropriate initial conditions at the core of the

smoothed string at $\bar{\rho} = 0$, $\Delta z = 0$, this ensures that no conical singularity forms at the core of the string.

Now that we have an expression for $\ddot{\Psi}_0$, we can evaluate the integrand for A_0 . As it turns out, the solution $\ddot{\Psi}_0 = \frac{\dot{\Psi}_0^2}{2\Psi_0}$ in Eq. (35) is precisely the condition for the vanishing of the integrand of A_0 . This leads us to the conclusion that for the class of portals we have considered here, the portal mouths experience no acceleration toward each other; the portal mouths neither attract nor repel, even when brought close together.

F. Curvature singularity formation

Since the absence of an effective force between the portal mouths indicates that classical general relativity presents no obstruction to their collision, one might conceivably imagine that the collision process results in topology change. A topology changing process will likely require the tearing of the manifold, and one might expect the formation of a curvature singularity as the portal mouths are brought together.

To see that a curvature singularity does indeed form, we analyze what happens to the Ricci scalar as the portal mouths are brought together. Consider the case where the portal mouths are approaching each other with some initial velocity given by some specification of initial data for Ψ . One might imagine that since Eq. (24) has a rather general form, the metric at a later time may be recast into the same form with a smaller value of z_0 and $\chi \sim 1$ at $\bar{\rho} = 0$. If in this case Ψ is of order unity, a significantly smaller value for z_0 will correspond to a decreased proper distance L [as defined in Eq. (25)] between the portal mouths. At $\bar{\rho} = 0$, the Ricci scalar takes the form:

$$\begin{aligned} R|_{\bar{\rho}=0} &= \frac{2\dot{\Psi}\Psi - \dot{\Psi}^2 - 2\Psi\partial_{\bar{\rho}}\partial_{\bar{\rho}}\Psi}{2\Psi^2} \\ &+ \frac{(\Psi+1)\chi\partial_z\Psi - 2(\Psi-1)\Psi\partial_z\chi}{\Delta z\chi^2\Psi^2} \\ &- \frac{2(\Psi-1)(\partial_z\lambda^2 + \chi - 1 - \Psi\dot{\lambda}^2)}{\Delta z^2\chi^2\Psi}. \end{aligned} \quad (37)$$

For points $|\Delta z| < z_0$, the last two terms in the Ricci scalar become large as $z_0 \rightarrow 0$. It is straightforward to show that $\partial_z\Psi \sim \frac{k_z}{z_0}$, with k_z of order unity. At the core of the string $\bar{\rho} = 0$, $\Delta z = 0$, one must have $\Psi = \alpha^2 = 4$ to ensure that the spatial geometry there remains locally flat. Though the boundary conditions for satisfying the junction conditions at $z = 0$ for the line element (24) are more complicated, one can still establish that the junction conditions require $\Psi = 1$ at $\bar{\rho} = 0$. Since $\Psi = 4$ at $z = z_0$ and $\Psi = 1$ at $z = 0$ along $\bar{\rho} = 0$, one concludes that for some value of $|\Delta z| < z_0$, $\partial_z\Psi \sim \frac{k_z}{z_0}$, with k_z of order unity.

Now at $z = 0$, one might also expect z derivatives to vanish since the geometry is symmetric about $z = 0$.

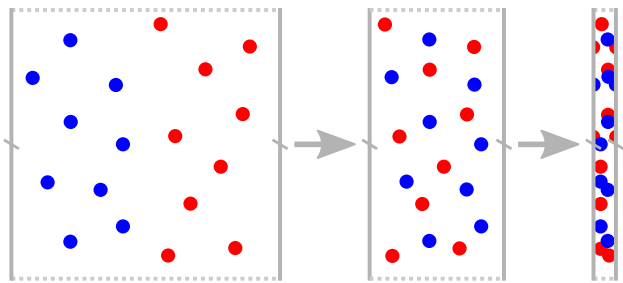


FIG. 8. An illustration describing the behavior of a rigid arrangement of cosmic strings between the portal mouths as the mouths approach each other (the leftmost diagram is earliest in time). Here, the z direction is horizontal, the radial direction is vertical, and the strings (indicated by the red and blue dots) are perpendicular to the page and parallel to the ϕ direction. The portal mouths correspond to the identified vertical lines. As the distance between the portal mouths decreases, the density of cosmic strings increases.

Since $\Psi = 1$ at $\bar{\rho} = 0$, and assuming that the dynamics preserve the symmetries ($\dot{\Psi} = \dot{\Psi} = 0$), the Ricci scalar simplifies to:

$$R|_{\bar{\rho}=z=0} = -\partial_{\bar{\rho}}\partial_{\bar{\rho}}\Psi. \quad (38)$$

In principle, the Ricci scalar at $\bar{\rho} = 0$, $z = 0$ may diverge in the $z_0 \rightarrow 0$ limit if $\partial_{\bar{\rho}}\partial_{\bar{\rho}}\Psi$ diverges.

Intuitively, the formation of a singularity in the Ricci curvature indicates that the density of anisotropic fluid becomes large as the portal mouths approach each other. To understand this, consider what happens to the matter between the portal mouths in the region $\bar{\rho} < a$, $|\Delta z| < z_0$ for finite a . In between the portal mouths, curves parallel to the z -axis (by which we mean curves of constant $t, \bar{\rho}, \phi$) have finite length on the order of the separation distance $z_0 \sim L$ between the portal mouths. As the portal mouths approach each other, the separation distance decreases, and it follows that the volume of the region between the portal mouths decreases. For smoothed cosmic strings, there will always be a finite amount of matter in the region $\bar{\rho} < a$, $|\Delta z| < z_0$, and it follows that the density of the matter must become large as the portal mouths approach each other. This mechanism is illustrated in Fig. 8, which depicts the anisotropic matter distribution between the portal mouths as a bundle of (low) negative mass cosmic strings.

VIII. CONCLUSION

We have described in detail the construction and topology of portals supported by smoothed matter distributions, and have obtained line elements, given in Eqs. (12) and (24) for a class of (large radius) axisymmetric portals supported by an anisotropic fluid. We have shown that the portal mouths experience no acceleration toward each other, which in turn suggests that there is no effective

force present between the portal mouths in the direction parallel to the axis of symmetry. We have also shown that the Ricci scalar diverges as the portal mouths collide, as one might expect. These results indicate that for the class of portal-type geometries considered, gravity alone does not prevent a collision between mouths of smoothed portals, and that, since the Ricci scalar diverges, a complete description of such a collision and the final state will likely require a theory of quantum gravity. Regardless, one might be able to make some progress toward understanding the aftermath of portal self-collisions by relaxing symmetry assumptions and considering the interactions of unsmoothed cosmic strings. The interaction of unsmoothed cosmic strings as described in [38,39] suggests that in general, the self-collision of asymmetric portal geometries in such a case will likely result in highly nontrivial spatial topologies and cosmic string configurations.

Our results are based on a simple classical matter model, that of an anisotropic fluid, in which the stresses for the smoothed cosmic string are simplified in that they are directed only along the length of the string, at least in the large a limit we have considered. Since there are no stresses in the directions perpendicular to the strings, the fluid does not contribute to the effective force between portal mouths. The lack of acceleration between the portal mouths arising from the solution to the Einstein equations indicates that gravity does not generate an effective force between the portal mouths. One might expect this to be the case if one imagines the anisotropic fluid to consist of a bundle of low (negative) mass/tension cosmic strings; since the geometry in the immediate region around a single unsmoothed cosmic string is locally flat, a collection of strings will not gravitate.

One might expect our results to change when quantum effects are included. In the region between the portal mouths $\rho < a$, $|\Delta z| < z_0$, curves parallel to the z -axis have topology S^1 , which suggests that quantum fields within this region must satisfy periodic boundary conditions. One may then expect the portal mouths to experience an attractive (topological) Casimir force when the portal mouths are separated by small distances (see 12.3.3 of [1] and also [40] for a discussion of the Casimir effect with periodic boundary conditions).

A more detailed matter model for the smoothed cosmic string could also produce an effective force between the portal mouths, changing our result. One might, for instance, consider an electrically charged cosmic string, which would produce a repulsion between the portal mouths if the overall charge is nonzero, or a neutral current-carrying string, which would attract, as the symmetry about $z = 0$ implies that the currents are parallel. It is also worth investigating whether strings with negative mass can be constructed in null energy condition-violating field theories, such as the Einstein-Dirac-Maxwell theory. A simple example involves the construction of negative mass strings from phantom fields, in which the action for the matter

sector for the fields has the opposite sign relative to the gravitational action. In the case of local gauge strings [41,42], one might imagine that in the long-distance limit (in which gravity is weak), their phantom counterparts interact similarly, as the actions differ only by an overall sign. From numerical studies of interacting local gauge strings [43], parallel oriented strings weakly repel, so one might expect a weak repulsion for phantom gauge strings.

These considerations indicate that the nature and strength of the interaction between portal mouths are not determined primarily by the gravitational interaction (as described by classical general relativity). Rather, the behavior of closely separated portal mouths depends critically on the behavior of matter—both the matter supporting the portals and the behavior of quantum fields

around portals can change the direction and magnitude of the effective force between the portal mouths. An interesting question, motivated by the singularity which forms as the portal mouths are brought together, is whether low-energy quantum gravitational effects, manifesting as higher-curvature terms in the effective action, introduce nontrivial gravitational interactions between the portal mouths.

ACKNOWLEDGMENTS

We thank Mark Baumann for helpful discussions. J. C. F. acknowledges financial support from FCT—Fundação para a Ciência e Tecnologia of Portugal Grant No. PTDC/MAT-APL/30043/2017 and Project No. UIDB/00099/2020.

-
- [1] M. Visser, *Lorentzian Wormholes: From Einstein to Hawking* (AIP Press, New York, 1995).
- [2] M. Visser, Traversable wormholes: Some simple examples, *Phys. Rev. D* **39**, 3182 (1989).
- [3] G. W. Gibbons and M. S. Volkov, Weyl metrics and wormholes, *J. Cosmol. Astropart. Phys.* **05** (2017) 039.
- [4] G. W. Gibbons and M. S. Volkov, Zero mass limit of Kerr spacetime is a wormhole, *Phys. Rev. D* **96**, 024053 (2017).
- [5] G. W. Gibbons and M. S. Volkov, Ring wormholes via duality rotations, *Phys. Lett. B* **760**, 324 (2016).
- [6] D. M. Zipoy, Topology of some spheroidal metrics, *J. Math. Phys.* (N.Y.) **7**, 1137 (1966).
- [7] S. V. Krasnikov, Quantum inequalities do not forbid spacetime shortcuts, *Phys. Rev. D* **67**, 104013 (2003).
- [8] M. Krasnikov, *Back-in-Time and Faster-than-Light Travel in General Relativity* (Springer, Berlin, 2018).
- [9] Portal, Valve Software (2007); Portal 2, Valve Software (2011).
- [10] J. A. Wheeler, Geons, *Phys. Rev.* **97**, 511 (1955).
- [11] C. W. Misner, K. S. Thorne, and J. A. Wheeler, *Gravitation* (Freeman, San Francisco, 1973).
- [12] S. W. Hawking, Spacetime foam, *Nucl. Phys.* **B144**, 349 (1978).
- [13] J. G. Cramer, R. L. Forward, M. S. Morris, M. Visser, G. Benford, and G. A. Landis, Natural wormholes as gravitational lenses, *Phys. Rev. D* **51**, 3117 (1995).
- [14] M. S. Morris and K. S. Thorne, Wormholes in spacetime and their use for interstellar travel: A tool for teaching general relativity, *Am. J. Phys.* **56**, 395 (1988).
- [15] M. S. Morris, K. S. Thorne, and U. Yurtsever, Wormholes, Time Machines, and the Weak Energy Condition, *Phys. Rev. Lett.* **61**, 1446 (1988).
- [16] J. L. Friedman, K. Schleich, and D. M. Witt, Topological Censorship, *Phys. Rev. Lett.* **71**, 1486 (1993).
- [17] D. Hochberg and M. Visser, Null Energy Condition in Dynamic Wormholes, *Phys. Rev. Lett.* **81**, 746 (1998).
- [18] J. L. Rosa, J. P. S. Lemos, and F. S. N. Lobo, Wormholes in generalized hybrid metric-Palatini gravity obeying the matter null energy condition everywhere, *Phys. Rev. D* **98**, 064054 (2018).
- [19] J. L. Blázquez-Salcedo, C. Knoll, and E. Radu, Traversable Wormholes in Einstein-Dirac-Maxwell Theory, *Phys. Rev. Lett.* **126**, 101102 (2021).
- [20] E.-A. Kontou and K. Sanders, Energy conditions in general relativity and quantum field theory, *Classical Quantum Gravity* **37**, 193001 (2020).
- [21] R. Geroch, Domain of dependence, *J. Math. Phys.* (N.Y.) **11**, 437 (1970).
- [22] C. W. Lee, Topology change in general relativity, *Proc. R. Soc. A* **364**, 295 (1978).
- [23] S. W. Hawking and G. F. R. Ellis, *The Large Scale Structure of Space-Time* (Cambridge University Press, Cambridge, England, 1973).
- [24] D. Deutsch, Quantum mechanics near closed timelike lines, *Phys. Rev. D* **44**, 3197 (1991).
- [25] H. D. Politzer, Simple quantum systems in spacetimes with closed timelike curves, *Phys. Rev. D* **46**, 4470 (1992).
- [26] A. Chamblin, G. W. Gibbons, and A. R. Steif, Kinks and time machines, *Phys. Rev. D* **50**, R2353 (1994).
- [27] U. Yurtsever, A remark on kinks and time machines, *Gen. Relativ. Gravit.* **27**, 691 (1995).
- [28] G. F. R. Ellis and B. G. Schmidt, Singular space-times, *Gen. Relativ. Gravit.* **8**, 915 (1977).
- [29] S. V. Krasnikov, Finite energy quantization on a topology changing spacetime, *Phys. Rev. D* **94**, 044055 (2016).
- [30] S. V. Krasnikov, String-like singularities taken seriously, *Proc. Sci.*, ISFTG2009 (2009) 014 [arXiv:0909.4963].
- [31] W. Israel, Singular hypersurfaces and thin shells in general relativity, *Nuovo Cimento B* **44**, 1 (1966); Erratum, *Nuovo Cimento B* **48**, 463 (1967).
- [32] E. Poisson, *A Relativist's Toolkit: The Mathematics of Black-Hole Mechanics* (Cambridge University Press, Cambridge, England, 2004).

- [33] A. Flachi and V. Vitagliano, Symmetry breaking and lattice kirigami: Finite temperature effects, *Phys. Rev. D* **99**, 125010 (2019).
- [34] M. Alcubierre, *Introduction to 3+1 Numerical Relativity* (Oxford University Press, Oxford, 2008).
- [35] T. Baumgarte and S. Shapiro, *Numerical Relativity: Solving Einstein's Equations on the Computer* (Cambridge University Press, Cambridge, England, 2010).
- [36] E.ourgoulhon, *3+1 Formalism in General Relativity: Bases of Numerical Relativity* (Springer-Verlag, Berlin, 2012).
- [37] <http://github.com/justincfeng/mathematica-files/blob/main/2021/Portal.nb>.
- [38] C. Hellaby, The gravitational interaction of conical strings, *Gen. Relativ. Gravit.* **23**, 767 (1991).
- [39] G. F. R. Ellis, Interacting cosmic strings, *Rendiconti Seminario Matematico, Torino* **50**, 25 (1992), <http://www.seminariomatematico.polito.it/rendiconti/cartaceo/50-1/25.pdf>.
- [40] S. A. Fulling, *Aspects of Quantum Field Theory in Curved Spacetime*, London Mathematical Society Student Texts Vol. 17 (Cambridge University Press, Cambridge, England, 1989), <https://doi.org/10.1017/CBO9781139172073>.
- [41] D. Garfinkle, General relativistic strings, *Phys. Rev. D* **32**, 1323 (1985).
- [42] P. Laguna-Castillo and R. A. Matzner, Discontinuity cylinder model of gravitating U(1) cosmic strings, *Phys. Rev. D* **35**, 2933 (1987).
- [43] R. A. Matzner, Interaction of U(1) cosmic strings: Numerical intercommutation, *Comput. Phys.* **2**, 51 (1988).